NORSAR

NORSAR Scientific Report No. 1-2000/2001

Semiannual Technical Summary

1 April - 30 September 2000

Frode Ringdal (ed.)

Kjeller, November 2000

6.2 Regional Seismic Threshold Monitoring

(Paper presented at the 22nd Annual Seismic Research Symposium)

We are starting a project to develop an optimized, automatic capability to monitor seismic events originating in an extended geographical region, using data from a sparse network of regional arrays and three-component stations. The work will build on the site-specific threshold monitoring technique developed under previous contracts. As an integral part of the method development, we plan to apply and evaluate the method in several practical applications. Our focus will be on using IMS and selected non-IMS stations to experimentally investigate the performance of regional threshold monitoring of a grid system covering the entire Novaya Zemlya region, and an area with high mining activity (e.g. the Kola Peninsula).

The basic approach in the project will be:

- To apply a regional travel time model for the paths between each station and grid node, possibly with source-station specific corrections.
- To apply wave attenuation relationships based primarily on regional calibration events, as available.
- To apply optimized bandpass filters for the grid nodes to be monitored, also considering the use of several bandpass filters in parallel if sufficient calibration information is not available.
- To provide automatic "explanation facilities" to assist the analyst in assessing the results

An important consideration in the project work will be to lay the foundation for its actual implementation in an operational monitoring system. Thus, the software will be developed using the general framework already provided by the prototype IDC, and the examples of applications will to a large extent (although not exclusively) be based on data from the emerging IMS. To facilitate a possible future implementation of this method in the IDC operational environment, the data formats will be made compatible with those of the global Threshold Monitoring system now operational at the Vienna International Data Centre.

Objective

The objective of this work has been to assess the applicability of a temporary three-component network for Threshold Monitoring (Kværna and Ringdal, 1999; Ringdal and Kværna, 1989, 1992) of a small mining area located within local/regional distances. In particular, we have focused on comparing the performance of such a network with the performance of a single IMS array with respect to background noise levels and suppression of signals from interfering events. These results will be important when considering strategies for permanent monitoring of a larger region.

Research Accomplished

Station network and data

In the time period May-October 1999, 13 Lennartz MARSlite data loggers equipped with three-component LE-3D/5s were deployed in Finnmark, northern Norway. The project was a cooperative project between NORSAR and the University in Potsdam, Germany, primarily initiated for studying the local seismicity of the neotectonic Masi fault system (Schweitzer, 1999).

This instrument deployment, denoted the “MASI network”, provided continuous data for the entire period of operation. A map with the sensor sites is shown in Fig. 6.2.1. Within the same area we also find the ARCES array (IMS station PS 28) and the IRIS three-component station Kevo (KEV) in northern Finland that is also a part of the finnish national seismic network. Continuous data from both ARCES and KEV were stored together with the data from the MASI network on CDs for subsequent analysis.

A quarry with an areal extent of approximately 2 km across is located on the Kola Peninsula, between the towns of Nikel and Zapolarnyi near the Russian-Norwegian border. Relatively large blasts (~100 tons) are regularly detonated in this quarry, providing strong signals at the nearby stations. An example of such an event as recorded at three of the MASI stations and at ARCES is shown in Figs. 6.2.2 and 6.2.3. Clear P- and S-, and Rg-phases are observed at many of the closest stations.

For the purpose of optimizing the SNR of the phases to be used for threshold monitoring, the three-component observations were rotated into the L, Q, and T ray oriented coordinate system, where P generally had the largest SNR in the L direction and S in the Q or T directions, as seen from Fig. 6.2.2. For ARCES, the best SNRs were found on array beams steered with either P or S velocities, But as seen from Fig. 6.2.3**,** where the center three-component ARA0 has been rotated into the L, Q, T coordinate system, the largest P amplitude is found on the L component and the largest S amplitude is found on the T component. Most of the P energy on the horizontal components is in this way projected into the L component. This effect will usually be observable for local and regional P phases where the rays approach the Earth’s surface at relatively large incidence angles.

For the purpose of testing the performance of the MASI network for monitoring of the quarry near Nikel, we derived processing parameters for Threshold Monitoring from the event shown in Figs. 6.2.2 and 6.2.3. This event had an announced yield of 98 tons and were assigned a local magnitude of 1.97 based on the S-phase recordings at ARCES and Apatity. Details on the processing parameters are given in Table 6.2.1.

Threshold monitoring of the mine near Nikel, Russia

In a practical monitoring situation, a variety of seismic stations at local distances may be available for monitoring a given target site of interest. Usually, such local networks are of a lower quality and sensitivity than IMS stations, but this is to some extent compensated for by the proximity of the network stations to the target site. This tradeoff is in fact one of the main topics for study under the present project.

The IMS network in Fennoscandia is composed of high-quality regional arrays. In addition, we have access to experimental data from local stations such as the MASI network, and this gives us the possibility to test the concept of optimized site-specific seismic monitoring using dense local networks and comparing the results to monitoring using a sparse network of high-quality seismic arrays.

We have carried out a monitoring experiment focusing on the mining site near Nikel, Kola Peninsula. Our purpose has been to compare the results from site-specific monitoring in the following two cases:

- Optimized threshold monitoring using P and S waves from the ARCES array
- Optimized threshold monitoring using P and S waves a local network composed of the MASI stations supplemented by the Kevo station in Finland

We note that the ARCES array is at a distance of about 200 km from the target site, whereas the local network stations are at distances ranging from 30 km to about 300 km. The closest station (MA05) should in theory be able to provide the best recording of mining events at Nikel. In practice, this station is not ideally situated, and its capability is therefore not quite as good as expected. We will return to this point in the following discussion.

Monitoring example for 2 June 1999

Figs. 6.2.4 and 6.2.5 show the results from optimized site-specific threshold monitoring for the two cases mentioned above (ARCES array and the local network) for a typical 24-hour period (2 June 1999). In the following, we provide some comments to these plots, which in fact illustrate many of the most important conclusions from this preliminary study:

The ARCES plot (Fig. 6.2.4) shows three traces: The two bottom traces correspond to the P-phase and the S-phase. We note that the threshold monitoring technique can be used on individual phases as well as on a combination of phases from one or several stations. In this particular case, the ARCES P-phase monitoring result shows a general “background” noise level of about magnitude 0. This simply means that the background noise level for an ARCES P-beam steered to the Nikel site, with an optimized filter setting, and compensated for wave attenuation, is close to magnitude 0. We can easily translate this to a detectability estimate, simply by adding a detection threshold (typically a factor of 4.0 in SNR, or 0.5 in magnitude units). In a detectability context, it would thus mean that the ARCES P-wave detectability for this site is around magnitude 0.5.

The S-phase plot for ARCES (Fig. 6.2.4) is interpreted in the same way as the P-wave trace. The background level for the S-phase is slightly lower than for the P-phase (about magnitude -0.5). This reflects the fact that the ARCES S-phase is stronger than the P-phase for events from this mine. We recall that the threshold monitoring trace shows the “upper limit” of an event that could possibly have occurred at a given instance in time. Thus the “absence” of an S-phase on the recorded trace is a stronger indication of a low upper limit than the “absence” of a P-phase.

The combined P and S threshold trace for ARCES (upper trace in Fig. 6.2.4) shows the overall threshold monitoring result using all the available information from the ARCES array. The background level is about magnitude -0.6, and the number of “spurious” peaks due to interfering events and other noise bursts is reduced compared to either the P-wave trace or the S-wave trace. The actual events at the mining sites, as well as the other main peaks on the trace, are indicated. Note that all the peaks exceeding magnitude 0 can be either associated with events in the mine or explained as a result of other causes. Thus, the monitoring capability of the ARCES array for the Nikel mining site is close to magnitude 0.

Fig. 6.2.5 is a threshold plot for the local network defined earlier. In this case, 5 station traces are shown (5 bottom traces), with the combined network trace on the top. Note that each of the 5 station traces have been generated using a combination of the P and S phase for that station, so that we have not displayed the individual phase traces in each case.

First we will briefly comment on the performance of the individual stations. The best station is the "permanent" station Kevo, which has a background threshold of about magnitude 0. Kevo is known to be an excellent station for local as well as regional/teleseismic recording, and is situated on hard rock in a low-noise environment. It is therefore not surprising that it is performing well, especially taken into account that the temporary MASI stations were, due to logistic considerations, placed near populated areas, and some also on sediments. Nevertheless, the performance of Kevo is encouraging. Compared to ARCES, KEV is at about the same distance from the target site (actually slightly nearer). The fact that ARCES has a better performance than KEV is not surprising, since the ARCES array has the advantage of noise suppression through beamforming of 25 sensors. This is sufficient to explain the performance difference of about 0.6 magnitude units.

For the stations in the MASI network, the most pronounced feature is the high variability of the background noise. While we have not attempted to study this in detail, we attribute it to the siting of the instruments and the proximity to man-made noise sources (roads, buildings etc.). Nevertheless, these stations have a threshold (background noise) between 0 and 1 on the magnitude scale, which means that they will contribute to lowering the overall network threshold. Thus, the combined thresholds (top of Fig. 6.2.5) is well below magnitude 0, although not quite as low as for the ARCES array. The number of spurious peaks is reduced compared to the ARCES plot, and this is in fact one of the main benefits of having a distributed network available rather than a concentrated array. The geographical distribution of the network enables spurious noise bursts or interfering signals to be more effectively suppressed.

Monitoring example for 17 August 1999

Our second example is from the day 17 August 1999 (Figs. 6.2.6 and 6.2.7). This is the day of the large Turkey earthquake (occurring early in the morning GMT), and during the same day (at about 4.40 GMT a relatively large earthquake occurred in Revda, Kola Peninsula. These "interfering" events naturally stand out on the plots, both for the ARCES array (Fig. 6.2.6) and the network (Fig. 6.2.7). Otherwise, the same considerations as were previously made for the 2 June example also apply in this case: The ARCES threshold is slightly lower than the network threshold, but the network has a reduced occurrence of spurious peaks ton the combined threshold trace.

We note that the closest network station (MA05) was not in operation on 17 August 1999. This seems to have had little effect on the network threshold. This is encouraging, since it indicates a robustness to failure of one or a few individual network stations.

Conclusions and recommendations

The main objective of the research described here is to develop and test a new, advanced method for applying regional seismic array technology to the field of nuclear test ban monitoring. To that end, we have addressed the development and testing of a method for optimized seismic monitoring of an extended geographical region, using a sparse network of regional arrays and three-component stations. We have applied the method to a temporary local network in northern Norway, and demonstrated that such a network can in certain cases be processed with a threshold monitoring capability that approaches that of a high-quality regional array (ARCES). We emphasize that the experiments undertaken so far addresses the monitoring of a

site that is within local distance (0-300 km) of the network, and that a high-quality regional array will become progressively more capable than the network as the distance from the network to the target site increases.

We believe that the results described in this paper as well as in earlier contributions demonstrate that the optimized threshold monitoring method has the potential to become an important tool in day-to-day monitoring of seismic activity. By this method, the full resources of the monitoring network will be brought to bear to focus on a specific target site in order to enable monitoring of this target site with as high a capability as the network and available calibration information will allow.

In future research we plan to develop the site-specific method further to enable monitoring of a larger area, and it will then be necessary to apply a number of "optimized" beams. This is simple in principle, but in practice, the number of such beams may easily become too large to be reasonably manageable by the analyst, calling for an additional level of data reduction. We will develop a semi-automated method to form a (potentially large) number of optimized beams to cover a given region, and to process jointly, by automatic means, the resulting threshold traces so as to provide the analyst with a suitable "composite" result for review. We believe that in this way the threshold monitoring technique can be developed into a powerful tool for practical seismic CTBT monitoring.

Acknowledgements

We would like to acknowledge Frank Krüger and Daniel Vollmer of the Institute for Geosciences at the University of Potsdam, Germany for their extensive support during planning and field work of the MASI experiment. The University of Potsdam also provided the 13 mobile stations of the temporary network.

T. Kværna
F. Ringdal
J. Schweitzer
L. Taylor

(Sponsored by The Defense Threat Reduction Agency, Arms Control Technology Division, Nuclear Treaties Branch)

References

Kværna, T. and F. Ringdal (1999): Seismic Threshold Monitoring for Continuous Assessment of Global Detection Capability, accepted for publication in BSSA.

Kværna, T., J. Schweitzer, L. Taylor and F. Ringdal (1999): Monitoring of the European Arctic using regional generalized beamforming. In: *NORSAR Semiannual Tech. Summ. 1 October 1998 - 31 March 1999, NORSAR Sci. Rep. 2-98/99*, Kjeller, Norway

Ringdal, F. & T. Kværna (1989): A multichannel processing approach to real time network detection, phase association and threshold monitoring, *Bull. Seism. Soc. Am.*, 79, 1927-1940.

Ringdal, F. & T. Kværna (1992): Continuous seismic threshold monitoring, *Geophys. J. Int.*, 111, 505-514.

Schweitzer, J. (1999): The MASI-1999 field experiment. In: *NORSAR Semiannual Tech. Summ. 1 April - 30 September 1999, NORSAR Sci. Rep. 1-1999/2000*, Kjeller, Norway

Table 6.2.1: Parameter processing for Threshold Monitoring of the mine near Nikel.

Station	Phase	Flow	Fhigh	Azimuth	Inc/ Vel	Comp	STA len	Travel time	STA calib	Dis-tance (km)
MA05	P	3.0	8.0	89.0	84.2	l	0.6	5.46	-2.016	27.58
MA05	S	3.0	8.0	89.0	-	t	0.5	8.86	-2.856	27.58
MA04	P	4.5	9.0	109.09	34.42	l	1.0	12.95	-0.835	59.01
MA04	S	3.0	6.0	110.23	60.87	t	1.0	17.76	-1.661	59.01
MA03	P	4.0	8.0	88.2	78.3	l	0.5	25.06	-1.283	146.50
MA03	S	4.0	8.0	88.2	78.3	t	1.0	42.33	-1.883	146.50
KEV	P	3.0	6.0	95.75	42.18	l	1.0	28.14	-1.308	150.40
KEV	S	3.0	8.0	110.17	63.70	t	1.0	45.14	-1.634	150.40
MA02	P	4.5	9.0	83.69	73.46	l	1.0	33.68	-1.447	199.96
MA02	S	3.5	7.0	124.06	62.56	t	1.0	57.54	-1.531	199.96
ARCES	P	4.0	8.0	92.70	7.99	z	1.0	34.75	-1.737	205.23
ARCES	S	4.0	8.0	94.12	4.81	z	1.0	60.31	-2.183	205.23
MA12	P	4.0	8.0	98.3	65.0	l	0.5	37.39	-1.728	225.01
MA12	S	4.0	8.0	98.3	65.0	q	1.5	64.23	-2.486	225.01
MA13	S	2.0	4.0	103.84	65.62	q	1.0	64.43	-1.221	225.11
MA06	P	3.5	8.0	126.99	27.72	l	1.0	41.00	-0.873	248.46
MA06	S	1.5	3.0	124.06	62.56	t	1.0	69.46	-1.198	248.46
MA10	P	2.0	5.0	71.63	60.18	l	1.0	46.57	-0.858	282.62
MA10	S	1.5	5.0	60.59	63.18	t	1.0	78.45	-1.305	282.62
MA08	P	4.0	8.0	75.0	53.0	l	1.0	49.01	-0.686	295.58
MA08	S	4.0	8.0	75.0	53.0	q	1.0	81.61	-1.210	295.58

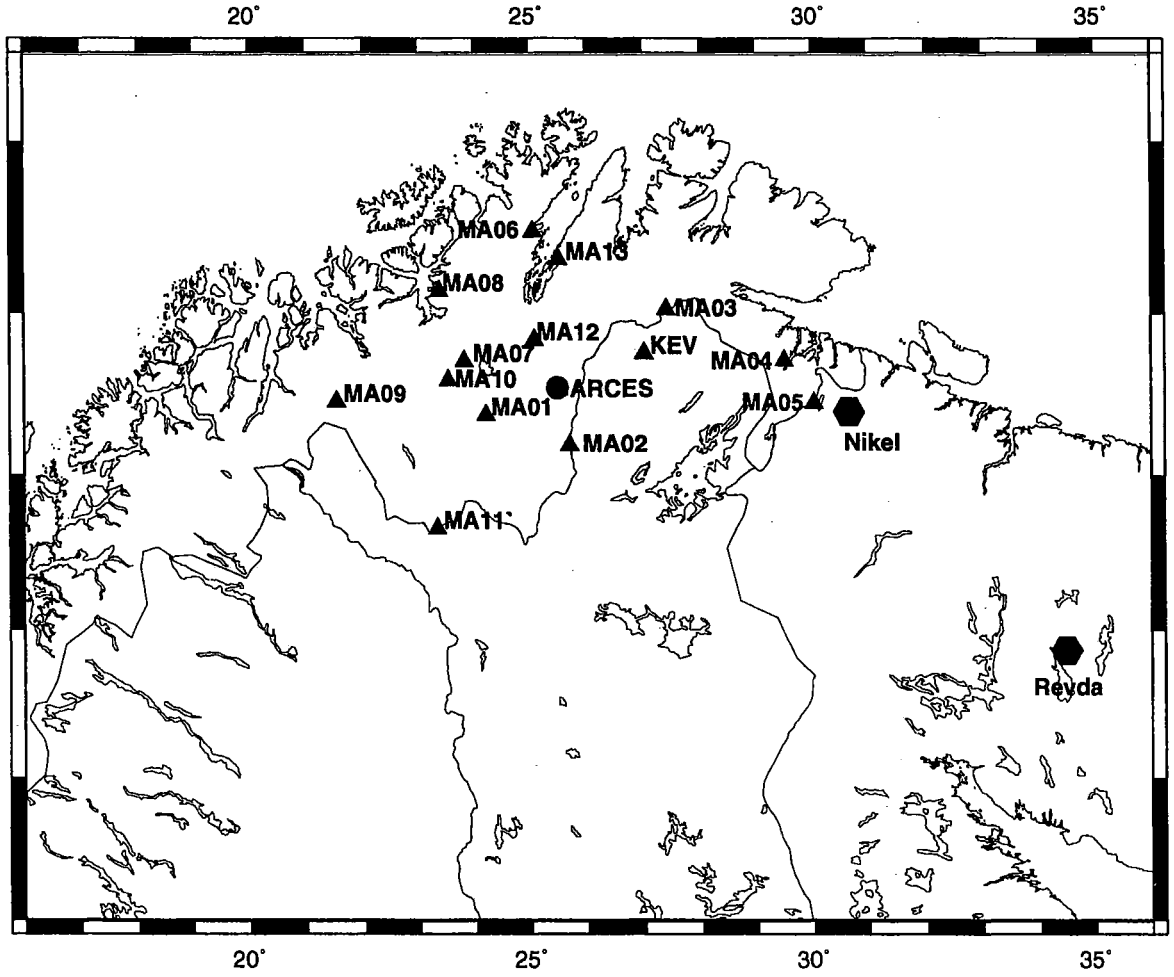

Fig. 6.2.1. Map showing the locations of the stations of the MASI network, the ARCES array, and the KEV station. Also shown are the locations of the quarry near Nikel and the epicenter of an M_s 4.2 earthquake occurring near Revda on the Kola peninsula.

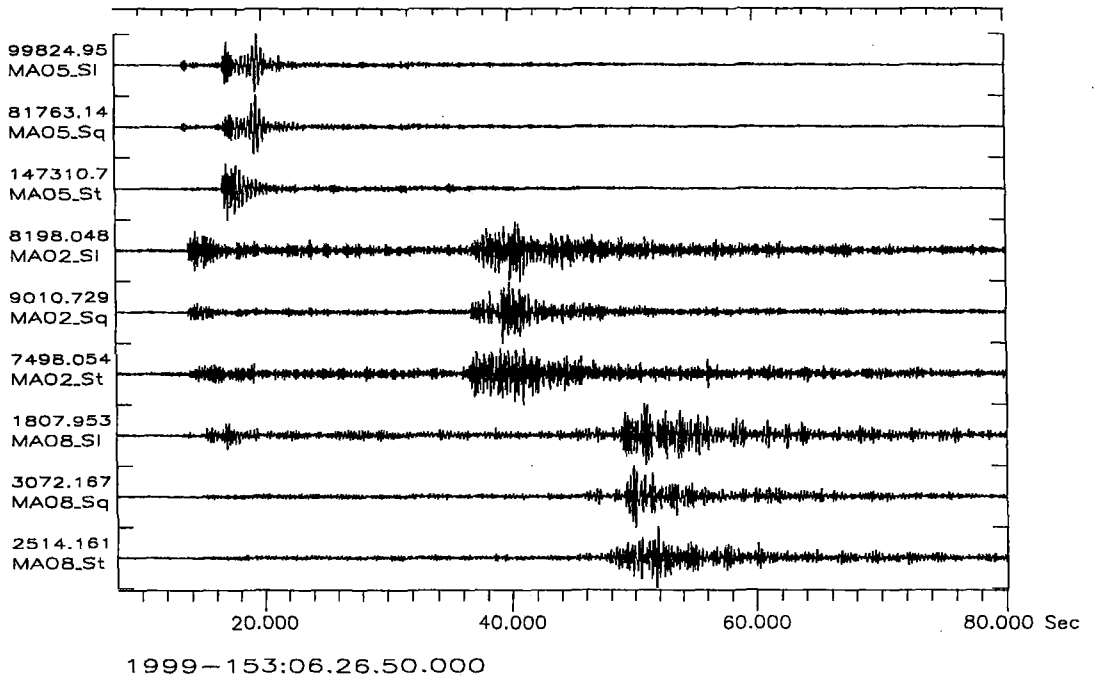

Fig. 6.2.2. Recordings of the quarry blast near Nikel (2 June1999, M_L 1.97) at three of the MASI stations. The traces were rotated into the L, Q, T components and bandpass filtered between 3 and 10 Hz.

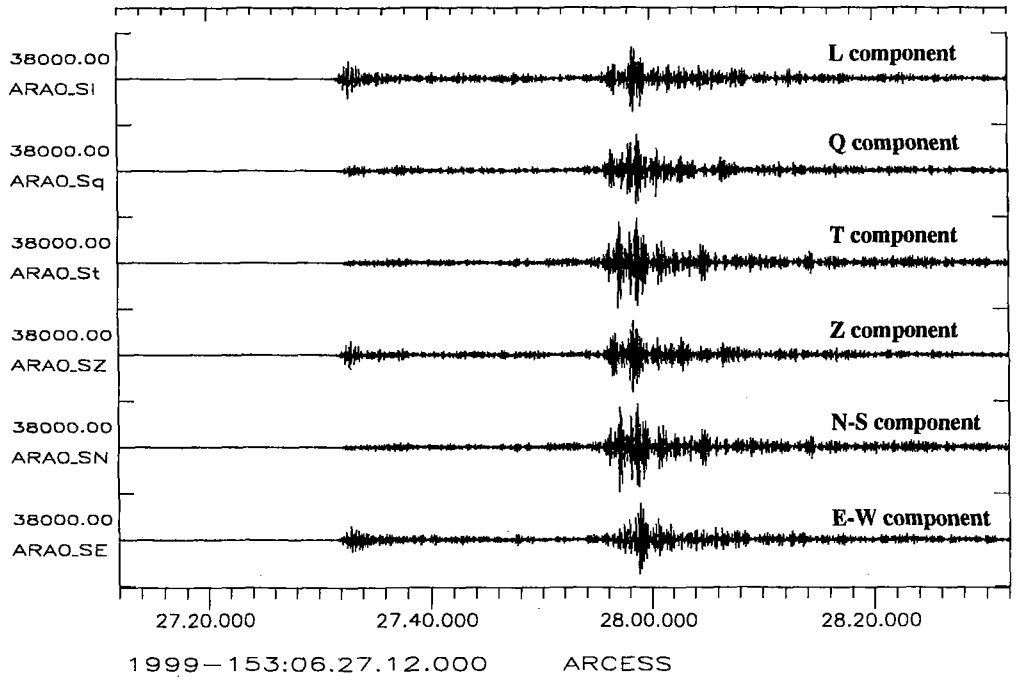

Fig. 6.2.3. Recordings of the quarry blast near Nikel (2 June1999, M_L 1.97) at ARA0, the central three-component element of the ARCES array. The upper three traces show the L, Q, T components and all traces were bandpass filtered between 4 and 10 Hz.

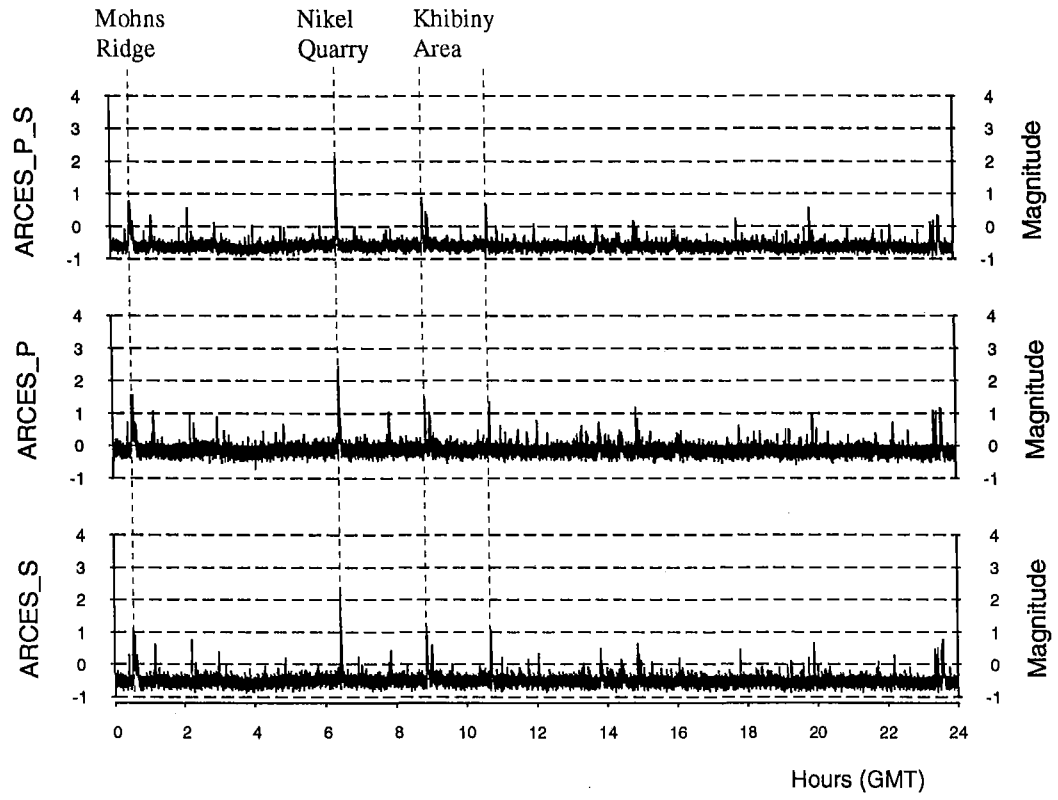

Fig. 6.2.4. Results from threshold monitoring of the quarry near Nikel for 2 June 1999, using the ARCES array. The combined P and S-phase threshold trace is shown on top, whereas the two lower traces show the thresholds for the P- and S-phases individually. The locations of the events causing the threshold peaks are given above the upper trace.

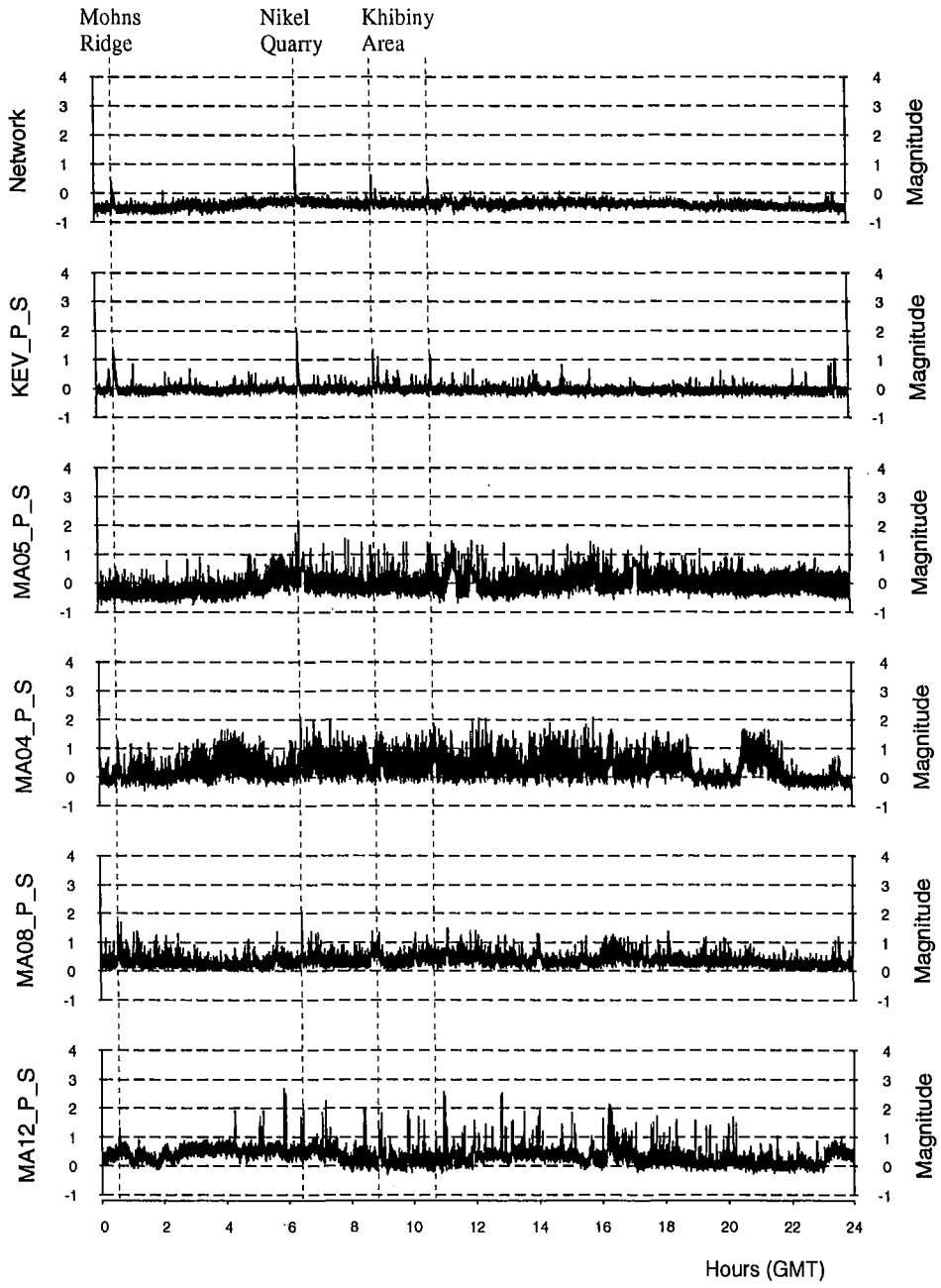

Fig. 6.2.5. Results from threshold monitoring of the quarry near Nikel for 2 June 1999, using the MASI network. The combined P and S-phase threshold trace for the network is shown on top, whereas the other traces show the combined P- and S-phase thresholds for selected stations. The locations of the events causing the threshold peaks are given above the upper trace.

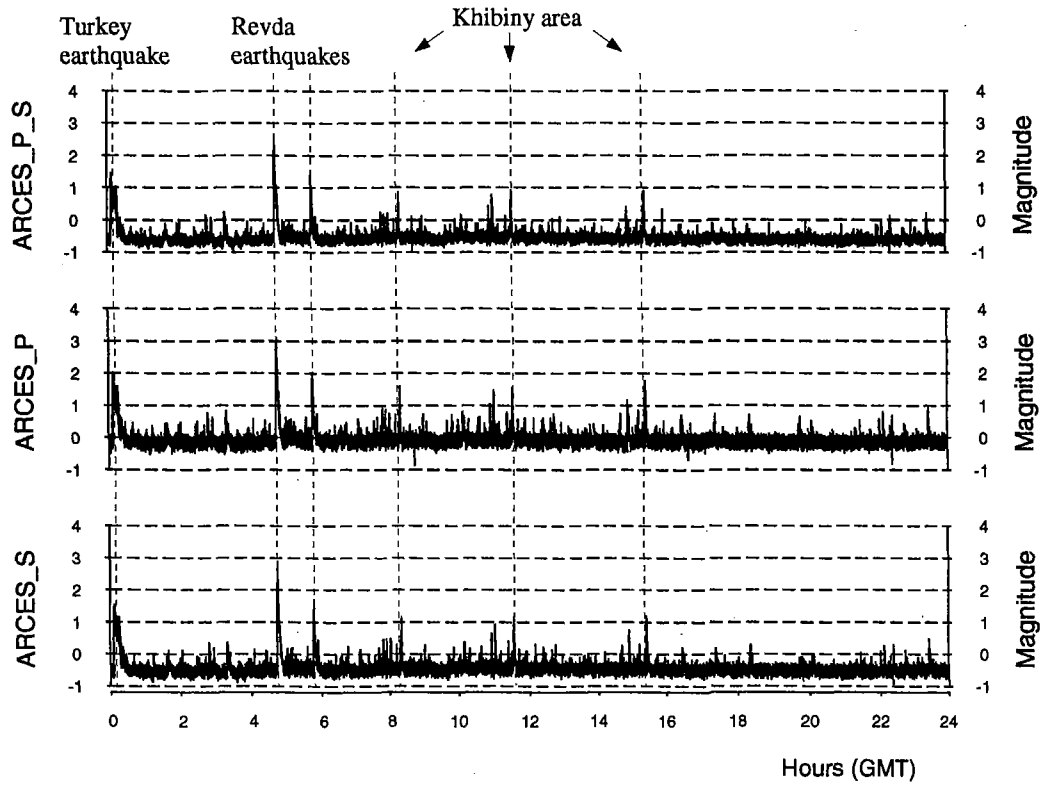

Fig. 6.2.6. Results from threshold monitoring of the quarry near Nikel for 17 August 1999, using the ARCES array. The combined P and S-phase threshold trace is shown on top, whereas the two lower traces show the thresholds for the P- and S-phases individually. The locations of the events causing the threshold peaks are given above the upper trace.

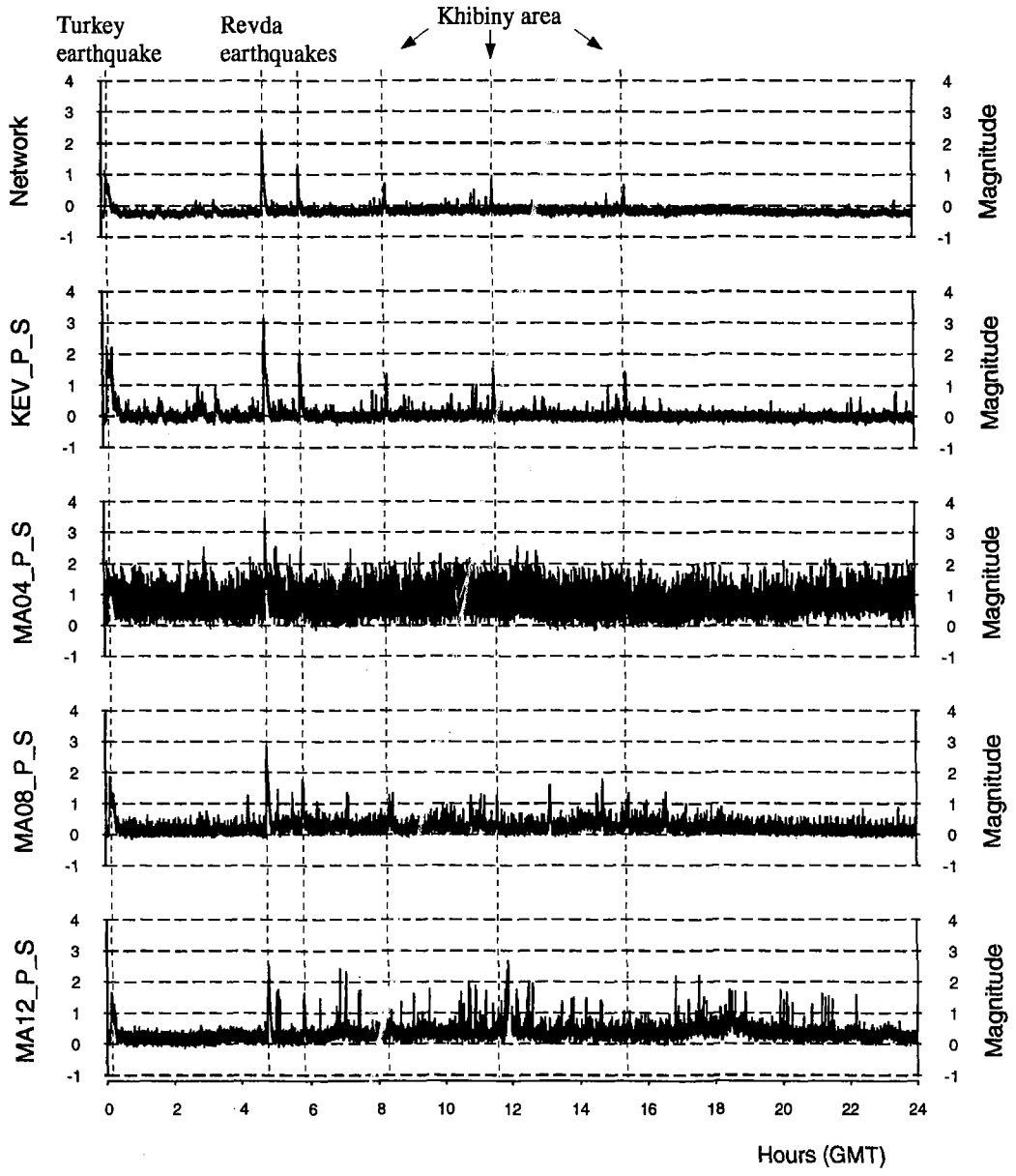

Fig. 6.2.7. Results from threshold monitoring of the quarry near Nikel for 17 August 1999, using the MASI network. The combined P and S-phase threshold trace for the network is shown on top, whereas the other traces show the combined P- and S-phase thresholds for selected stations. The locations of the events causing the threshold peaks are given above the upper trace.